

Apparent Luminosity Function and Statistical Properties of Fast Radio Bursts

L. B. Li^{1,2}, Y. F. Huang^{1,2,*}, Z. B. Zhang³, D. Li^{4,5}, B. Li^{1,6}

hyf@nju.edu.cn

Received _____; accepted _____

¹School of Astronomy and Space Science, Nanjing University, Nanjing 210046, China;
hyf@nju.edu.cn

²Key Laboratory of Modern Astronomy and Astrophysics (Nanjing University), Ministry of Education, Nanjing 210046, China

³Department of Physics, College of Sciences, Guizhou University, Guiyang 550025, China

⁴National Astronomical Observatories, Chinese Academy of Sciences, Beijing 100012, China

⁵Key Laboratory for Radio Astronomy, Chinese Academy of Sciences, China

⁶Institute of High Energy Physics, Chinese Academy of Sciences, Beijing 100049, China

ABSTRACT

Fast Radio Bursts (FRBs) are intense radio flashes from the sky that are astonishingly characterized by millisecond durations and Jansky-level flux densities. Only 16 FRBs have been reported in the literature till now. We carry out a statistical analysis on these events. Their mean dispersion measure, after subtracting the contribution from the interstellar medium of our Galaxy, is found to be $\sim 655 \text{ pc cm}^{-3}$, strongly supporting the idea that they are of cosmological origin. Their energy release in radio band spans about three orders of magnitude, with a mean value of $\sim 6.42 \times 10^{38} \text{ ergs}$. The radio energy is found to be positively correlated with the observed fluence and the dispersion measure excess, and the fluence also shows a clear positive correlation with the FRB duration. Among all these events, FRBs 010621 and 010724 seem to form a distinct group in a few plots, indicating that there may be at least two classes of FRBs. More interestingly, although the FRB study is still in a very early phase, the already considerable number of FRBs enables us to derive a useful luminosity function for them, i.e., $dN/dF_{\text{obs}} = (4400 \pm 400)F_{\text{obs}}^{-1.18 \pm 0.15} \text{ sky}^{-1} \text{ day}^{-1}$, where F_{obs} is the observed radio fluence in units of Jy ms. We notice that the power-law index of 1.18 is significantly less than the expected value of 3/2 for homogeneous sources in a flat Euclidean space. Based on this luminosity function, it is estimated that the Chinese Five-hundred-meter Aperture Spherical radio Telescope will be able to detect about 5 FRBs for every 1000 hours of observation time.

Subject headings: pulsars: general – stars: neutron – radio continuum: general – intergalactic medium – methods: statistical

1. Introduction

Fast Radio Bursts (FRBs) are intense radio flashes that occur randomly in the sky. Till the end of January 2016, sixteen FRBs have been discovered as the originally unexpected outcomes of fast radio transient surveys (Lorimer et al. 2007; Keane et al. 2012; Thornton et al. 2013; Burke-Spolaor & Bannister 2014; Spitler et al. 2014; Champion et al. 2015; Masui et al. 2015; Petroff et al. 2015; Ravi et al. 2015). Most FRBs were detected at ~ 1400 MHz by the Parkes telescope (14 detections) or the Arecibo telescope (1 detection), and only one burst (FRB 110523) was detected at ~ 800 MHz by the Green Bank Hydrogen Telescope (GBT). FRBs are characterized by their strong brightness (≥ 1 Jy), but with very short durations ($\sim ms$). There are no clear observational indications that FRBs can occur repeatedly from the same direction. Their counterparts have not been observed at other wavelengths though a few very limited follow-up searching campaigns have been carried out (e.g. Petroff et al. 2015), which makes the nature of these peculiar bursts even more enigmatic. The arrival time of an FRB at different wavelength is characterized by a frequency-dependent delay of $\Delta t \propto \nu^{-2}$, and the pulse width is found to scale as $W_{\text{obs}} \propto \nu^{-4}$ (Lorimer et al. 2007; Thornton et al. 2013). Both characteristics are consistent with the expectations for radio pulses propagating through a cold, ionized plasma. These facts strengthen the view that FRBs are of astrophysical origin, but not interferences from the Earth.

The dispersion measure (DM), defined as the line-of-sight integral of the free electron number density, is a useful indication for distance. An outstanding feature of FRBs is that their dispersion measures are very high, much larger than the contribution from the electrons in our Galaxy. The measured DMs of known FRBs range from 375 pc cm^{-3} to 1629 pc cm^{-3} , while the expected contributions from the Galaxy and the potential host galaxy are typically much less than $\sim 100 \text{ pc cm}^{-3}$. Lorimer et al. (2007) and Thornton et al.

(2013) suggested that the high DM is dominated by the contribution from the ionized intergalactic medium (IGM). It implies that FRBs may occur at cosmological distances. With their large DMs, FRBs then potentially may be a powerful probe for studying the IGM and the spatial distribution of free electrons.

The millisecond duration of FRBs suggests that the sources should be compact, and the high radio brightness requires a coherent emission mechanism (Katz 2014a; Luan & Goldreich 2014). Since FRBs’ redshifts are estimated to be in a range of $z \sim 0.5$ — 1 (Thornton et al. 2013; Champion et al. 2015), the energy release at radio wavelengths can be as high as $\sim 10^{39}$ — $\sim 10^{40}$ ergs. The progenitors and the physical nature of FRBs are currently unknown. Many possible mechanisms have been proposed, such as supergiant pulses from pulsars (Cordes & Wasserman 2015), collapses of hypermassive neutron stars into black holes (Falcke & Rezzolla 2014; Ravi & Lasky 2014), evaporating black holes (Rees 1977), magnetar giant flares (Kulkarni et al. 2014; Lyubarsky 2014; Pen & Cornor 2015), collisions of asteroids with neutron stars (NS) (Geng & Huang 2015), some special kinds of gamma-ray bursts (Zhang 2014), interaction of planetary companions with the magnetic fields of pulsars (Mottez & Zarka 2014), or double neutron stars mergers (Totani 2013). Multi-wavelength observations of FRBs and their counterparts seem necessary to discriminate these models.

People are eagerly hoping to detect much more FRBs in the near future. The event rate of FRBs and the observation power of our radio telescopes then become two major factors being involved. Thornton et al. (2013) have argued that if FRBs happens in the sky isotropically, their actual event rate could be as high as $\sim 10^4 \text{ sky}^{-1} \text{ day}^{-1}$. Hassall, Keane & Fender (2013) discussed the prospects of detecting FRBs with the next-generation radio telescopes and suggested that the Square Kilometer Array (SKA) could detect about one FRB per hour. Based on the redshifts estimated from the measured

DMs, Bera et al. (2016) went further to study the FRB population and predicted that the upcoming Ooty Wide Field Array¹ can detect FRBs at a rate of $\sim 0.01 — 10^3$ per day. Note that their predicted detection rate is in a very wide range, which mainly stems from the large uncertainty of FRB event rate in the sky.

Sixteen FRBs have been observed till the end of January 2016. This number is already considerable and the currently available samples can be used to do some statistic researches. Since the redshifts of FRBs are not directly measured, but are hinted from their DMs, the reliability of these redshifts still needs to be clarified. In this study, we use the directly measured fluences of FRBs to derive an apparent luminosity function for them. We then use the luminosity function to estimate the observable event rate of FRBs by the Chinese Five-hundred-metre Aperture Spherical radio Telescope (FAST) which is expected to begin to operate in September 2016 (Nan et al. 2011). Some statistic results are also derived for FRBs. Our article is organized as follows. In Section 2, we briefly describe the sample of 16 FRBs. Statistical analyses of their parameters are presented in Section 3. In Section 4, we derive the apparent luminosity function of FRBs. In Section 5, the observational prospect of FRBs with FAST is addressed. Our conclusions and discussion are presented in Section 6.

2. Samples and Data

As of January 2016, the number of FRBs reported is 16, of which 14 bursts were discovered by Parkes, one burst (FRB 121002) was detected by Arecibo, and the most recently reported one (FRB 110523) was by GBT. All these FRBs were generally observed in radio bands around 1400 MHz, except that FRB 110523 was detected at 700 — 900

¹<http://rac.ncra.tifr.res.in/>

MHz (Masui et al. 2015). A very detailed catalogue of known FRBs have been compiled by Petroff et al. (2016) and the data are available online².

For our study, we have collected some key parameters of all the FRBs available, and the data are listed in Table 1 (also see Huang & Geng (2015) for a similar data table but with fewer samples). Column 1 of Table 1 provides the FRB names. The observed width or duration of the corresponding radio pulse (W_{obs}) is presented in Column 2. When the radio emission passes through an ionized plasma, the narrow pulse will be broadened due to the scattering effect. In the simplest case, the pulse width increases as $W_{\text{obs}} \sim \sqrt{W_{\text{Int}}^2 + \tau_s^2}$, where W_{Int} is the intrinsic width and τ_s is the typical scattering time-scale (Hassall, Keane & Fender 2013; Narayan 1992; Rickett 1990). The W_{Int} of eight FRBs have been reported directly in the literature and are listed in Column 3. Column 4 is the observed peak flux density (S_{peak}) of each FRB. Columns 5 tabulates the observed fluences (F_{obs}) in units of Jy ms, which is calculated as $F_{\text{obs}} = S_{\text{peak}} \times W_{\text{obs}}$. Usually an FRB is assumed to be at the beam center at its detection, so the fluence may generally be the lower limit (Champion et al. 2015).

Columns 6, 7, and 8 of Table 1 present the observed DMs of FRBs, the DM contributions from the Galaxy (DM_{Galaxy}), and the DM excesses (DM_{Excess}), respectively. The DM excess is defined as $DM_{\text{Excess}} = DM - DM_{\text{Galaxy}}$. Following usual operations, we estimate the distances of FRBs from the DM excess as $z = (DM_{\text{Excess}} - 100 \text{ pc cm}^{-3})/1200 \text{ pc cm}^{-3}$ (Inoue 2004; Ioka 2003), where 100 pc cm^{-3} is an assumed contribution from the host galaxy (Huang & Geng 2015). With the estimated redshifts (Column 9), we then can calculate the corresponding luminosity distances (D_L) and the emitted radio energies (E_{radio}), which are presented in Columns 10 and 11, respectively. A Λ CDM cosmology with $H_0 = 71 \text{ km s}^{-1} \text{ Mpc}^{-1}$, $\Omega_m = 0.27$, and $\Omega_\Lambda = 0.73$ is adopted in our calculations. Note

²<http://astronomy.swin.edu.au/pulsar/frbcat/>

that the energies are derived based on a solid beaming angle of 1 sr (Thornton et al. 2013; Huang & Geng 2015). If the emission is isotropic, the energy involved will be $4\pi E_{\text{radio}}$. Finally, the references for each FRB event are presented in Column 12.

3. Statistical Analyses

We first focus on the distribution of the observed DMs of FRBs. Fig. 1 illustrates the histogram of DMs (Panel a) and DM excesses (Panel b). The observed DM spans a range of $200 - 1800 \text{ pc cm}^{-3}$, roughly in a normal distribution. Both the DM and the DM excess distribution can be well fitted with a Gaussian function. The DM Gaussian function peaks at $\sim 700 \text{ pc cm}^{-3}$, while DM_{Excess} peaks at $\sim 655 \text{ pc cm}^{-3}$, which accounts for $\sim 90\%$ of the mean DM. Panel (c) of Fig. 1 shows the histogram of the radio energy releases of the 16 FRBs, which follows a log-normal distribution. The range of E_{radio} is between 0.03×10^{39} ergs and 6.93×10^{39} ergs, and the mean energy is 6.42×10^{38} ergs, which is roughly consistent with that estimated by Huang & Geng (2015).

In Fig. 2, we plot some parameters such as the observed peak flux density, the fluence, the radio energy, and the Galaxy contribution rate of DM against the DM excess. Fig. (2a) shows that the peak flux density (S_{peak}) does not have any clear correlation with DM_{Excess} , which is somewhat unexpected since a more distant source usually tends to be dimmer. We suggest that the reason may be that the currently observed DM_{Excess} values are still in a relatively narrow range (the largest DM_{Excess} is only ~ 7 times that of the smallest one). However, note that a very weak tendency that FRBs with a larger DM_{Excess} seem to have a smaller S_{peak} still can be seen. In the future, more observed samples may make this tendency more obvious. Similarly, Fig. (2b) shows that the fluence (F_{obs}) does not correlate with DM_{Excess} . It indicates that the width of FRBs also does not depend on DM_{Excess} , this will be further shown in the following figures. In Fig. (2c), we see that E_{radio} shows a

strong correlation with DM_{Excess} , which is natural since E_{radio} has a square dependence on the distance. In fact, the best fit result of Fig. (2c) is $E_{\text{radio}} \propto DM_{\text{Excess}}^{2.61 \pm 1.11}$. The power-law index here is roughly consistent with the square relation, although with a still quite large error box). Fig. (2d) shows that as the “distance” increases, the contribution of our Galaxy in the total DM decreases, which is again a natural expectation. The best fit line in this panel corresponds to $DM_{\text{Galaxy}}/DM \propto DM_{\text{Excess}}^{-2.27 \pm 0.60}$.

In Fig. 3, we plot various parameters versus the observed and intrinsic pulse width of FRBs. Panels (3a) and (3b) show that the peak flux density (S_{peak}) does not correlate with either the observed width (W_{obs}) or the intrinsic width (W_{Int}). A clear correlation between the fluence and the observed width can be seen in Panel (3c), with a best fit result of $F_{\text{obs}} \propto W_{\text{obs}}^{0.97 \pm 0.37}$. With the power-law index being very close to 1, this correlation mainly reflects the definition that $F_{\text{obs}} = S_{\text{peak}} \times W_{\text{obs}}$ under the condition that S_{peak} is independent of W_{obs} as revealed in Panel (3a). Panel (3d) shows that when the pulse width is corrected for IGM scattering, the correlation between the fluence and the width still exists. The best fit result now gives a much smaller power-law index, i.e., $F_{\text{obs}} \propto W_{\text{Int}}^{0.18 \pm 0.07}$. Note that FRB 010724 seems to be an outlier as compared with other FRBs, thus is not included in the fitting in Panel (3d). Finally, we note that both E_{radio} and DM_{Excess} do not correlate with either W_{obs} or W_{Int} . Note that while the observed pulse width is relatively clustered, the spread in E_{radio} is as large as three orders of magnitude.

Fig. 4 illustrates the radio energy release versus the fluence. These two parameters are closely correlated except for FRBs 010621 and 010724. If not including these two events, all the other samples can be well fit with a power-law function of $E_{\text{radio}} \propto F_{\text{obs}}^{1.46 \pm 0.73}$. The derived power-law index is roughly consistent with the expected value of 1 within the 1σ range. FRBs 010621 and 010724 seem to be two distinct outliers in the plot. We argue that this may be an emerging clue indicating that FRBs might be divided into two groups. In

fact, in Figs. (2b), (3d), and (3g), we have marked the positions of these two events, which also show that they seem to be quite different from others.

4. Apparent Luminosity Function

An absolutely scaled luminosity function can be helpful to address the nature of FRBs (Bera et al. 2016). However, since the redshifts of FRBs have not been directly measured, but are only inferred from the DM excess, the derived absolute luminosity and energy releases of FRBs are thus still controversial (Katz 2014b; Luan & Goldreich 2014; Pen & Connor 2015). On the other hand, the apparent intensity distribution function of astronomical objects can provide helpful information on their nature. A good example is the study of gamma-ray bursts (GRBs). Before the redshifts of GRBs were directly measured, a deviation from the $-3/2$ power-law function in the peak flux distribution of GRBs was noted (Tavani 1998). It was explained as a hint for the cosmological origin of GRBs, which was later proved from direct redshift measurements. In this section, we will derive an apparent luminosity function from the currently available 16 FRBs.

We focus on the observed fluences (F_{obs}) of FRBs, but not simply the peak flux density. The reason is that radio sources can be seriously affected by scatter and scintillation of IGM, which makes the peak flux density relatively unstable. The combination of F_{obs} and S_{peak} , i.e. the fluence, can then more reliably indicate the fierceness of FRBs. Another reason is that due to the limited time resolving power of our radio receivers, an FRB should last long enough to be recorded so that the duration is also a key factor. In fact, a tentative cumulative distribution vs. the fluence has been drawn by Katz (2015) based on a smaller data set constituted of 10 FRBs.

As usual, we assume that the actual number density of FRBs occurring in the whole sky

per day at a particular fluence F_{obs} follows a power-law dependence, i.e. $dN/dF_{\text{obs}} = A F_{\text{obs}}^{-\alpha}$, where A is a constant coefficient and α is the power-law index. Both A and α need to be determined from observations. Note that A is in the units of events $\text{sky}^{-1} \text{day}^{-1}$. As a first step, we group the observed 16 FRBs into different fluence bins, with a bin width of ΔF . We count the number of FRBs in each bin and fit the data to get a best-fit power-law function for dN/dF_{obs} . In the upper panel of Fig. 5, we show our fitting result when the bin width is taken as $\Delta F = 2.5 \text{ Jy ms}$. In this case, we get the power-law index as $\alpha = 1.02 \pm 0.14$.

Obviously, since the total number of FRBs is still very limited, the choice of the bin width will seriously affect the fitting result. So, we have tried various bin width ranging from 0.5 Jy ms to 6 Jy ms to study the effect. For these different bin widths, the derived power-law indices are illustrated in the lower panel of Fig. 5. From this figure, we see that when the bin width is very small ($\Delta F \leq 2 \text{ Jy ms}$), the derived α depends strongly on the bin width. The reason is that in these cases, at most only two or three FRBs are grouped into one bin, thus the fluctuation dominates the final results. On the other hand, when the bin width is too large ($\Delta F > 4 \text{ Jy ms}$), the derived α also depends strongly on the bin width and the error box correspondingly becomes larger. Again the result is due to the fluctuation. In these cases, only two or three bins are left with a non-zero number of FRBs so that the derived α becomes unreliable. On the contrary, when ΔF is in the range of 2.5 — 4 Jy ms, the best-fit α keeps to be somehow constant and the error box is also small. So we choose such a ΔF range to derive the α parameter. To reduce the effect of fluctuation as far as possible, we calculate the mean value of α when ΔF is set as 2.5, 3.0, 3.5, 4.0 Jy ms, respectively, which finally gives $\alpha = 1.18 \pm 0.15$. Note that the derived power-law index is significantly less than $3/2$, the value expected for isotropic sources distributed homogeneously in a flat Euclidean space.

Now the task is to determine the coefficient of A in the luminosity function of $dN/dF_{\text{obs}} = AF_{\text{obs}}^{-\alpha}$. This could be done by considering the FRB detection rate reported by various FRB survey campaigns. To do this, we first integrate the luminosity function to get the actual event rate above a given fluence limit in the whole sky per day, which is

$$R(F_{\text{obs}} > F_{\text{Limit}}) = A \int_{F_{\text{Limit}}}^{F_{\text{max}}} F_{\text{obs}}^{-\alpha} dF_{\text{obs}}, \quad (1)$$

where F_{Limit} is the lowest threshold of a radio telescope and F_{max} is the upper limit of the fluence of observed FRBs, which is set as 35 Jy ms according to our current samples (the observed maximum fluence is ~ 32 Jy ms at present).

A few constraints on the actual event rate of FRBs have been provided by various FRB survey campaigns. Thornton et al. (2013) have proposed that if FRBs occur in the sky isotropically, the observable event rate of FRBs is $10^4 \text{ sky}^{-1} \text{ day}^{-1}$ for a fluence limit of 3 Jy ms. It indicates $R(F_{\text{obs}} > 3 \text{ Jy ms}) = 10^4 \text{ sky}^{-1} \text{ day}^{-1}$. With the detection of FRB 121102 with Arecibo, Spitler et al. (2014) have given $R(F_{\text{obs}} > 0.35 \text{ Jy ms}) = 3.1 \times 10^4 \text{ sky}^{-1} \text{ day}^{-1}$. Keane & Petroff (2015) suggested that the Parkes FRB rate above 2 Jy ms is $\sim 2500 \text{ sky}^{-1} \text{ day}^{-1}$. Law et al. (2015) reported a rate of $\leq 1.2 \times 10^4 \text{ sky}^{-1} \text{ day}^{-1}$ above a fluence limit of 1.8 Jy ms based on their observations. Rane et al. (2016) argued that at 1.4 GHz radio band, the all-sky event rate for FRBs above 4.0 Jy ms is $\sim 4.4 \times 10^3 \text{ sky}^{-1} \text{ day}^{-1}$. Recently, Champion et al. (2015) found five new FRBs in the archive data, and suggested that the event rate is $\sim 6000 \text{ sky}^{-1} \text{ day}^{-1}$ above a fluence limit of $\sim 0.13 - 5.9$ Jy ms.

Combining all these observational indications and using our Eq. (1), we can derive the coefficient as $A = (4.4 \pm 0.4) \times 10^3 \text{ sky}^{-1} \text{ day}^{-1}$. With the derived A and α parameters, we finally get the apparent luminosity function as,

$$\frac{dN}{dF_{\text{obs}}} = (4.4 \pm 0.4) \times 10^3 F_{\text{obs}}^{-1.18 \pm 0.15} \text{ sky}^{-1} \text{ day}^{-1}, \quad (2)$$

where F_{obs} is in units of Jy ms.

5. Prospects for FAST

FAST (Nan et al. 2011; Li et al. 2013), an ambitious Chinese megascience project, is currently being built in Guizhou province in the southwestern of China. With a geometrical diameter of 500 meters and an effective diameter of ~ 300 meters at any particular moment, it will be the largest single-dish radio telescope in the world when it comes into operation in September of 2016. FAST’s receivers will cover both low frequency (70-500 MHz) and middle frequency (0.5-3 GHz) bands. We here consider the prospect of detecting FRBs with FAST by using the derived apparent luminosity function. Below, our calculations are done at the L band (1400 MHz) of FAST, which should be the most favorable wavelength for FRB observations.

The sensitivity or the limiting flux density (S_{limit}) of a radio telescope can be estimated as (Zhang et al. 2015),

$$S_{\text{limit}} \simeq (12\mu\text{Jy}) \left(\frac{0.77 \times 10^3 \text{m}^2/\text{K}}{A_e/T_{\text{sys}}} \right) \left(\frac{S/N}{3} \right) \left(\frac{1\text{hour}}{\Delta\tau} \right)^{1/2} \left(\frac{100\text{MHz}}{\Delta\nu} \right)^{1/2}, \quad (3)$$

where T_{sys} is the system temperature, $\Delta\tau$ is the integration time, $\Delta\nu$ is the bandwidth, S/N is the signal-to-noise ratio which is usually taken as 10 for a credible detection of a FRB (Champion et al. 2015), A_e is the effective area and it equals to $\eta_A \pi (d/2)^2$, with η_A being the aperture efficiency and d being the illuminated diameter. FAST has a system temperature of $T_{\text{sys}} \sim 25K$ at 1400 MHz. For other parameters of FAST, we take $d = 300$ m, $\eta_A = 0.65$ (Zhang et al. 2015), $\Delta\nu = 300$ MHz, $\Delta\tau = 3$ ms (Law et al. 2015). The limiting fluence of FAST is then calculated to be $F_{\text{Limit}} = S_{\text{limit}} \times \Delta\tau = 0.03$ Jy ms. Note that from Equations (1) and (2), the actual FRB event rate above the fluence limit of 0.03 Jy ms is $(3.33 \pm 0.66) \times 10^4$ sky $^{-1}$ day $^{-1}$.

The beam size of a radio telescope is $\Omega \sim \pi\theta^2$, where $\theta \sim 1.22(\lambda/d)$ is the half opening angle of the beam. For FAST, the beam size is $\Omega \sim 0.008$ deg 2 at 1400 GHz. FAST has 19

beams so that the total instantaneous field-of-view (FoV) is 0.15 deg^2 . Considering all these parameters, we can get the daily detection rate of FRBs by FAST as,

$$R_{\text{FAST}} \sim (3.33 \pm 0.66) \times 10^4 \times \frac{0.15 \text{ deg}^2}{41253 \text{ deg}^2} \text{ day}^{-1} = 0.121 \pm 0.024 \text{ day}^{-1}. \quad (4)$$

For a 1000 hours of observation time, this will correspond to 5 ± 1 detections.

6. Discussion and Conclusions

Sixteen FRBs have been discovered in the archival survey data until 2016 January. In this study, we collect the available data of all published FRBs, and present a statistical analysis. The observed DM peaks at $\sim 700 \text{ pc cm}^{-3}$ and spans a range of 200 — 1800 pc cm^{-3} , while the DM excess peaks at $\sim 655 \text{ pc cm}^{-3}$ and accounts for $\sim 90\%$ of the total DM. The emitted radio energy spans about three orders of magnitude, with the mean energy being about $6.42 \times 10^{38} \text{ ergs}$. While most of the parameters do not correlate with each other, a clear correlation between the radio energy release and the DM excess has been found to be $E_{\text{radio}} \propto DM_{\text{Excess}}^{2.61 \pm 1.11}$ (Fig. 2c), which may reflect the square dependence of E_{radio} on the distance. The energy release also correlates with the observed fluence as $E_{\text{radio}} \propto F_{\text{obs}}^{1.46 \pm 0.73}$ (Fig. 4), roughly consistent with a linear expectation. It is also found that the observed fluence shows a clear and tight correlation with the duration of FRBs (Figs. 3c and 3d). From these statistical analyses, we found that FRBs 010621 and 010724 are quite different from others in several aspects. We argue that they may form a distinct group, indicating that there might be at least two classes of FRBs.

Using the observed fluence as an indication for the strength of FRBs and combining the constraints on the event rate of FRBs from various observational searches, we derive an apparent luminosity function for FRBs as $dN/dF_{\text{obs}} = (4.4 \pm 0.4) \times 10^3 F_{\text{obs}}^{-1.18 \pm 0.15} \text{ sky}^{-1} \text{ day}^{-1}$. Based on this expression, we were able to estimate the detection rate of FRBs by China's

coming FAST telescope. FAST typically has a sensitivity of 0.03 Jy ms when observing FRBs. With its 19 beams of L-band focal plane systems, FAST will have a total instantaneous FoV of 0.15 deg^2 . As a result, there will be roughly 1 detectable event every 10 days for FAST and 5 expected detections for every 1000 hours of observation time.

For standard candles that distribute isotropically and homogeneously in a flat Euclidean space, their observed intensity distribution should follow a power-law function with an index of $3/2$. We notice that the derived index of $\alpha = 1.18 \pm 0.15$ for FRBs is significantly less than $3/2$. It seems to indicate a deficiency of the dimmest FRBs, which is consistent with the tendency emerging from earlier studies (Katz 2015; Bera et al. 2016). There are a few factors that could lead to such a deviation. First, the total number of currently observed FRBs is still very limited. It can result in a large fluctuation in the measured power-law index. In fact, Caleb et al. (2015) have estimated that at least ~ 50 FRBs are needed to extract conclusive information on the physical nature of FRBs. Second, FRBs may not be strict standard candles, their brightness may distribute in a relatively wide range. But as long as the characteristics of FRBs does not evolve systematically with the distance, the index will not be affected too much. A wider brightness range will only result in a larger error box for α , which can still be reduced by increasing the FRB samples. Third, FRBs may not be homogeneous sources, the co-moving density or their brightness may evolve in space. For example, the co-moving FRB density may be smaller when the distance increase, or farther FRBs may not be as fierce as those nearer to us. Fourth, the space may not be a flat Euclidean space, e.g. for a curved Λ -CDM cosmology. In this case, the deviation of α from $3/2$ can be used as a probe for the cosmology (Caleb et al. 2015). Finally, it should also be noted that the apparent deficiency of the dimmest FRBs could also be due to the selection effect. Much weaker FRB events may actually have happened in the sky, but we were not able to record them or find them due to current technical limitations. To make clear which of the above factors has led to the smaller α , more new FRB samples would be

necessary in the future.

The possibility that there may be at least two kinds of FRBs also deserves further investigating. Spectrum information can be helpful in studying the classification, but unfortunately all current FRBs were observed only in a relatively narrow band. In future studies, broad-band observations should be conducted. Also, searching for the counterparts of FRBs at other wavelength (including gravitational waves), looking for the “afterglows”, and directly measuring the redshifts will also help to clarify the classification.

As addressed above, the apparent luminosity function derived here is still a preliminary result. We need much more samples to determine the power-law index more accurately. With an enormous effective area for collecting radio emissions, the Chinese FAST telescope is very suitable for FRB observations. It may be able to increase the FRB samples at a rate of ~ 10 events per year (assuming an effective observation time of 2000 hours). More importantly, FAST can operate in a very wide frequency range and can hopefully provide detailed spectrum information for FRBs. It is expected to be a powerful tool in the field.

This study was supported by the China Ministry of Science and Technology under State Key Development Program for Basic Research (973 program, Grant Nos. 2014CB845800, 2012CB821802), the National Natural Science Foundation of China (Grant Nos. 11473012, U1431126, 11263002) and the Strategic Priority Research Program (Grant No. XDB09010302).

REFERENCES

Bera, A., Bhattacharyya, S., Bharadwaj, S., Bhat, N. D. R., & Chengalur, J. N. 2016, arXiv:1601.05410

Burke-Spolaor, S., & Bannister, K. W. 2014, *ApJ*, 792, 19

Caleb, M., Flynn, C., Bailes, M. et al. 2015, arXiv:1512.02738

Champion, D. J., Petroff, E., Kramer, M. et al. 2015, arXiv:1511.07746

Cordes, J. M., & Wasserman, I. 2015, arXiv:1501.00753

Dolag, K., Gaensler, B. M., Beck, A. M., & Beck, M. C. 2015, *MNRAS*, 451, 4277

Falcke, H., & Rezzolla, L. 2014, *A&A*, 562, A137

Geng, J. J. & Huang, Y. F. 2015, *ApJ*, 809, 24

Hassall, T. E., Keane, E. F., & Fender, R. P. 2013, *MNRAS*, 436, 371

Huang, Y. F., & Geng, J. J. 2015, in Proceedings of “Frontiers in Radio Astronomy and FAST Early Sciences Symposium 2015 (FRA 2015)”, conference hold in Guiyang, China in July 2015 (arXiv:1512.06519)

Inoue, S. 2004, *MNRAS*, 348, 999

Ioka, K. 2003, *ApJL*, 598, L79

Katz, J. I. 2014a, *PhRvD*, 89, 103009

Katz, J. I. 2014b, arXiv:1409.5766

Katz, J. I. 2015, arXiv:1505.06220

Keane, E. F., & Petroff, E. 2015, *MNRAS*, 447, 2852

Keane, E. F., Stappers, B. W., Kramer, M., & Lyne, A. G. 2012, MNRAS, 425, L71

Kulkarni, S. R., Ofek, E. O., Neill, J. D., Zheng, Z., & Juric, M. 2014, ApJ, 797, 70

Law, C. J., Bower, G. C., Burke-Spolaor, S. et al. 2015, ApJ, 807, 16

Li, D., Nan, R., & Pan, Z. 2013, IAU Symposium, 291, 325, ed. J. van Leeuwen (arXiv:1210.5785)

Lorimer, D. R., Bailes, M., McLaughlin, M. A., Narkevic, D. J., & Crawford, F. 2007, Sci, 318, 777

Luan, J., & Goldreich, P. 2014, ApJL, 785, L26

Lyubarsky, Y. 2014, MNRAS, 442, L9

Mottez, F., & Zarka, P. 2014, A&A, 569, A86

Masui, K., Lin, H., Sievers, J. et al. 2015, Natur, 528, 523

Nan, R. D., Li, D., Jin, C. J. et al. 2011, IJMPD, 20, 989

Narayan, R. 1992, RSPTA, 341, 151

Pen, U.-L., & Connor, L. 2015, ApJ, 807, 179

Petroff, E., Bailes, M., Barr, E. D. et al. 2015, MNRAS, 447, 246

Petroff, E., Barr, E. D., Jameson, A. et al., 2016, arXiv:1601.03547

Rane, A., Lorimer, D. R., Bates, S. D. et al. 2016, MNRAS, 455, 2207

Ravi, V., & Lasky, P. D. 2014, MNRAS, 441, 2433

Ravi, V., Shannon, R. M., & Jameson, A. 2015, ApJ, 799, L5

Rees, M. J. 1977, *Natur*, 266, 333

Rickett, B. J., 1990, *ARA&A*, 28, 561

Spitler, L. G., Cordes, J. M., Hessels, J. W. T. et al. 2014, *ApJ*, 790, 101

Thornton, D., Stappers, B., Bailes, M. et al. 2013, *Sci*, 341, 53

Totani, T. 2013, *PASJ*, 65, L12

Zhang, B. 2014, *ApJL*, 780, L21

Zhang, Z. B., Kong, S. W., Huang, Y. F., Li, D., & Li, L. B. 2015, *RAA*, 15, 237

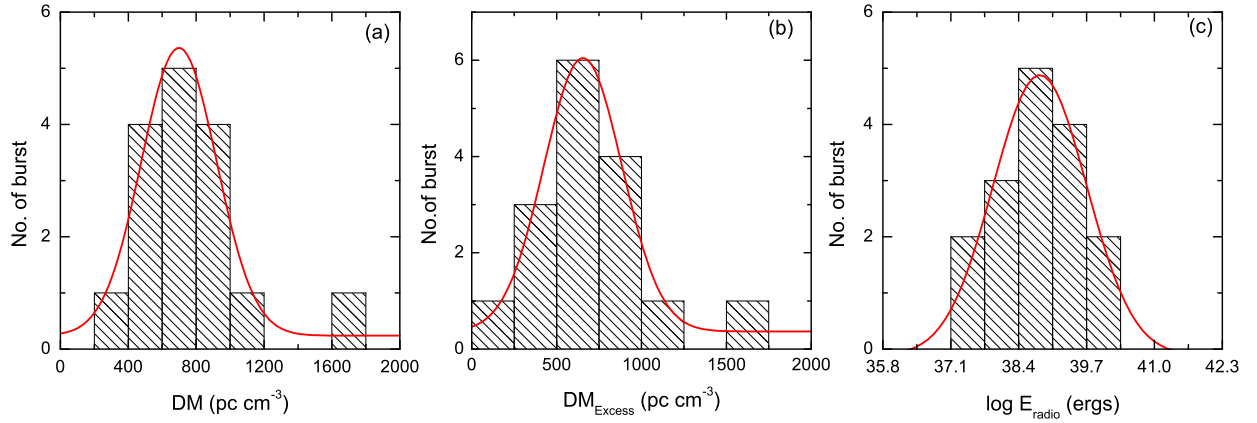


Fig. 1.— Histograms summarizing the distribution of the DM (Panel a), the DM excess (Panel b), and the radio energy release (Panel c). The solid curve in each panel is the best-fit Gaussian function.

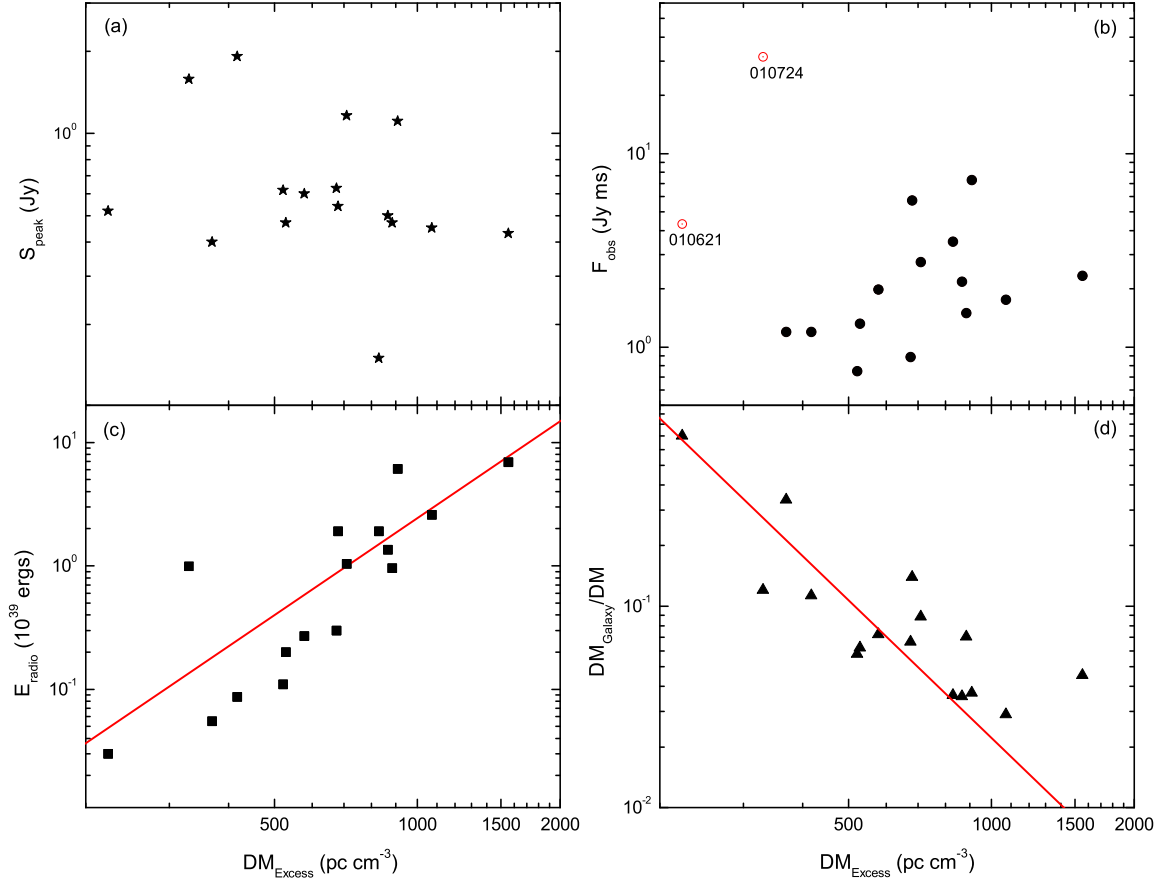


Fig. 2.— Some intensity parameters of FRBs vs. the DM excess. Panels (a), (b), and (c) illustrate the observed peak flux density, the fluence, and the radio energy, respectively. Panel (d) presents the Galaxy contribution rate of DM against the DM excess. The best fit lines are shown in Panels (c) and (d), when the two parameters are clearly correlated.

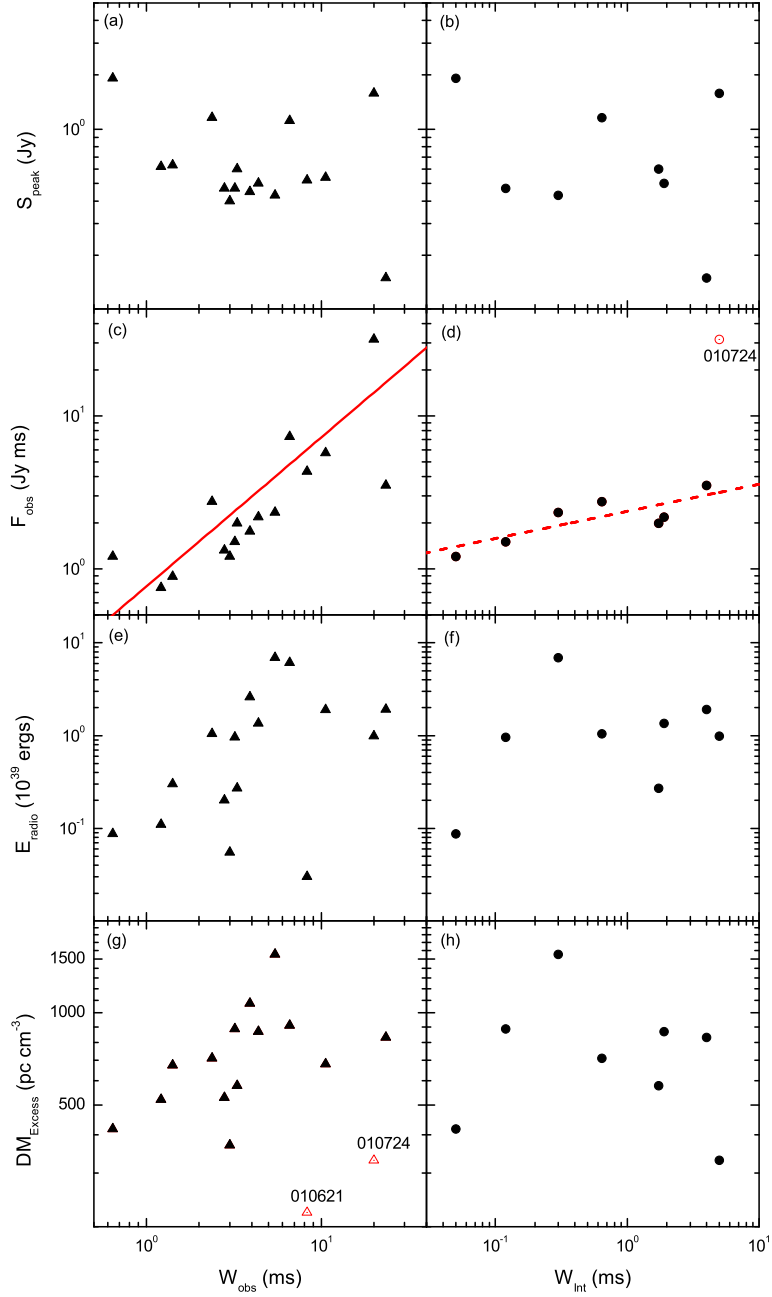


Fig. 3.— Various parameters vs. the observed pulse width (W_{obs} , the left column) and the intrinsic pulse width (W_{Int} , the right column) of FRBs. Panels (a) and (b) illustrate the peak flux density; Panels (c) and (d) illustrate the observed fluence; Panels (e) and (f) illustrate the radio energy release; Panels (g) and (h) illustrate the DM excess. The best fit lines are shown in Panels (c) and (d), when the two parameters are clearly correlated.

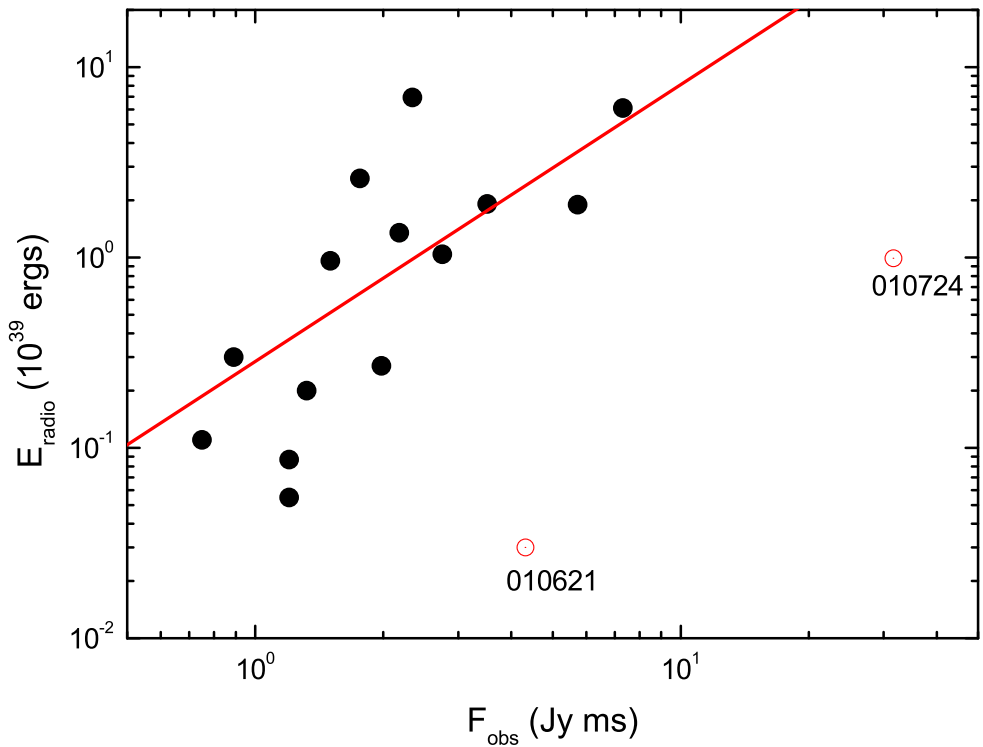


Fig. 4.— The radio energy release vs. the observed fluence for all FRBs. The solid line corresponds to the best fit result for observational data points, but not including FRBs 010621 and 010724. These two events seem to be distinct outliers as compared with others, indicating that they may form another group.

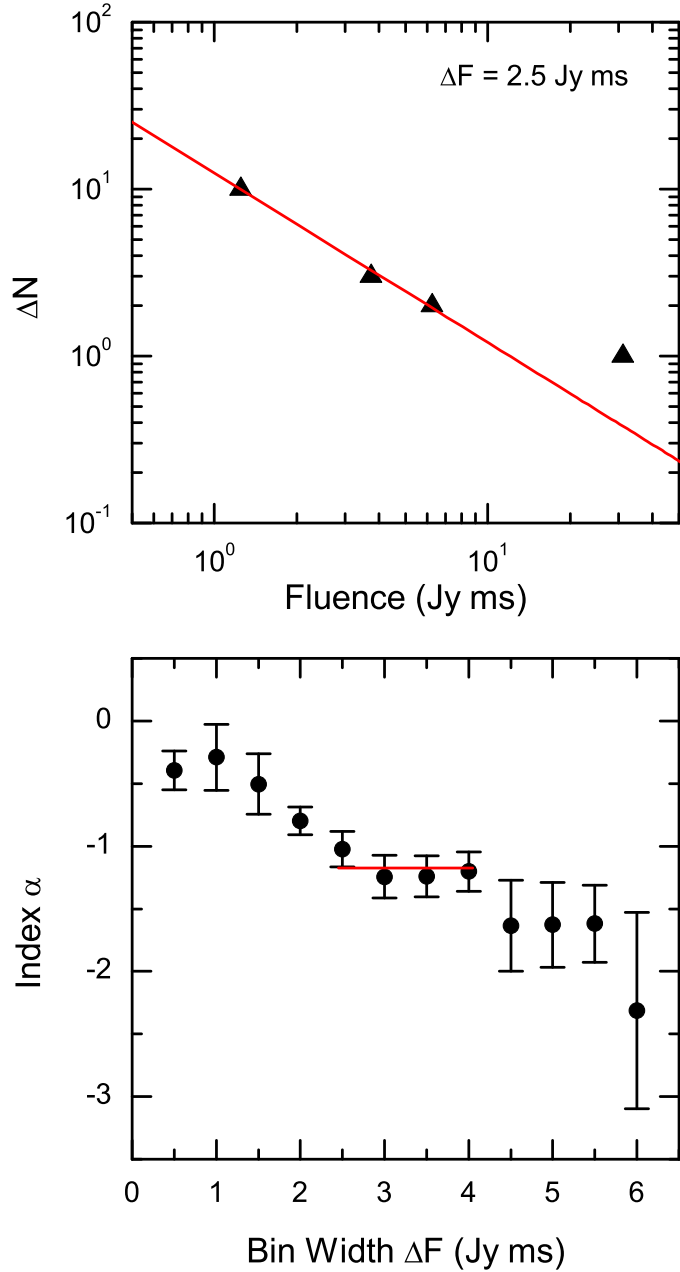


Fig. 5.— The distribution function of the observed fluence. The upper panel shows the distribution of FRBs when a bin width of $\Delta F = 2.5$ Jy ms is assumed, with the Y-axis showing the number of FRBs in each bin. The solid line corresponds to the best fit power-law function with an index of $\alpha = 1.02 \pm 0.14$. The lower panel illustrates the best fit α values when different bin widths are assumed, in which the short horizontal line shows the mean value of α for ΔF being in the range of 2.5 Jy ms $\leq \Delta F \leq 4.0$ Jy ms.

Table 1: Key parameters of 16 FRBs discovered to date. For a more detailed catalogue of the data, see Petroff et al. (2016).

FRB	W_{obs}	$W_{\text{int}}^{\text{a}}$	S_{peak}	F_{obs}	DM^{b}	DM_{Galaxy}	$DM_{\text{Excess}}^{\text{c}}$	z	D_{L}	$E_{\text{radio}}^{\text{d}}$	Ref. ^e
	(ms)	(ms)	(Jy)	(Jy ms)	(pc cm $^{-3}$)	(pc cm $^{-3}$)	(pc cm $^{-3}$)		(Gpc)	(10 39 ergs)	
(1)	(2)	(3)	(4)	(5)	(6)	(7)	(8)	(9)	(10)	(11)	(12)
010125	10.6	...	0.54	5.72	790	110	680	0.48	2.7	1.9	[1,3,4,6,10]
010621	8.3	...	0.52	4.32	746	523	223	0.1	0.45	0.03	[3,4,5,6,10]
010724	20	5	1.58	31.6	375	45	330	0.19	0.92	0.99	[3,4,6,7,10]
090625	4.36	1.9	0.50	2.18	899.6	32	867.6	0.64	3.71	1.35	[2,10]
110220	6.59	...	1.11	7.31	944	35	909	0.67	4.0	6.1	[3,4,6,10,13]
110523	3.3	1.73	0.60	1.98	623	45	578	3.04	2.1	0.27	[8,10]
110626	1.41	...	0.63	0.89	723	48	675	0.48	2.7	0.3	[3,4,6,10,13]
110703	3.9	...	0.45	1.76	1104	32	1072	0.81	5.1	2.6	[3,4,6,10,13]
120127	1.21	...	0.62	0.75	553	32	521	0.32	1.8	0.11	[3,4,6,10,13]
121002	5.44	0.3	0.43	2.34	1629	74	1555	1.21	8.19	6.93	[2,10]
121102	3.00	...	0.40	1.20	557	188	369	0.22	1.1	0.055	[4,10,12]
130626	3.20	0.12	0.47	1.50	952.4	67	885.4	0.65	3.78	0.96	[2,10]
130628	0.64	0.05	1.91	1.22	469.9	53	416.9	0.26	1.27	0.087	[2,10]
130729	23.4	4	0.15	3.51	861	31	830	0.61	3.48	1.91	[2,10]
131104	2.37	0.64	1.16	2.75	779	69	710	0.51	2.9	1.04	[3,4,10,11]
140514	2.8	...	0.47	1.32	563	35	528	0.36	1.9	0.20	[3,4,6,9,10]

^aThe intrinsic width of pulse.

^bThe dispersion measure.

^cThe dispersion measure excess, which is $DM - DM_{\text{Galaxy}}$.

^dThe emitted radio energy, assuming a solid beaming angle of 1 sr.

^eReferences.— [1] Burke-Spolaor & Bannister (2014); [2] Champion et al. (2015); [3] Dolag et al. (2015); [4] Huang & Geng (2015); [5] Keane et al. (2012); [6] Keane & Petroff (2015); [7] Lorimer et al. (2007); [8] Masui et al. (2015); [9] Petroff et al. (2015); [10] Petroff et al. (2016); [11] Ravi et al. (2015); [12] Spitler et al. (2014); [13] Thornton et al. (2013).